JOURNAL OF THERMOPHYSICS AND HEAT TRANSFER
Vol. 24, No. 3, July–September 2010

Thermal Performance of Microencapsulated Phase-Change-Material Slurry: Laminar Flow in Circular Tube

T. El Rhafiki,* T. Kousksou,† and Y. Zeraouli†
University of Pau, 64013 Pau Cedex, France

DOI: 10.2514/1.48707

A physical model for laminar forced-convection heat transfer of microencapsulated phase-change-material suspension in a circular tube with constant heat flux has been presented in this paper. Suspensions of aqueous solution and water microcapsules are tested. The energy equation is formulated by taking into consideration the heat absorption due to the phase change process. The physical model was validated with the results available in the literature. The influence of various factors is analyzed in detail.

Nomenclature

c	=	heat capacity, $J \cdot kg^{-1} \cdot K^{-1}$
D	=	tube diameter, m
f	=	liquid fraction
h	=	local heat transfer coefficient, $W \cdot m^{-2} \cdot K^{-1}$
h_p	=	heat transfer coefficient between the particle and the working fluid, $W \cdot m^{-2} \cdot K^{-1}$
k	=	thermal conductivity, $W \cdot m^{-1} \cdot K^{-1}$
L	=	length, m
L_F	=	latent heat of melting of the ice, $J \cdot kg^{-1}$
Pe	=	Peclet number
q_w	=	total heating rate, W
q''_w	=	wall heat flux, $W \cdot m^{-2}$
R	=	radius of circular tube, m
Re	=	Reynolds number
r	=	microcapsule radial coordinate, m
r_i	=	radius of phase change material core, m
r_p	=	radius of particle, m
r_s	=	radius of solid–liquid interface in particle, m
S	=	heat source
Ste	=	Stefan number
T	=	temperature, K
T_{wx}	=	dimensionless wall temperature
t	=	time, s
t^*	=	dimensionless time
u	=	velocity in axial direction, $m \cdot s^{-1}$
u_m	=	average velocity in axial direction, $m \cdot s^{-1}$
V	=	volume, m^3
X_E	=	eutectic concentration
X_{ic}	=	ice mass fraction
x	=	axial coordinate of circular duct, m
x_0	=	initial concentration
x^*	=	dimensionless axial coordinate of circular duct
y	=	radial coordinate of circular duct, m
α	=	thermal diffusivity, $m^2 \cdot s^{-1}$
ε	=	volume fraction of microencapsulated particles
ρ	=	density, $kg \cdot m^{-3}$
μ	=	dynamic viscosity, $Pa \cdot s^{-1}$
χ	=	fractional transformation

Subscripts

a	=	antifreeze
E	=	eutectic
e	=	effective
f	=	fluid
i	=	initial/inlet
ic	=	ice
p	=	particle
pcm	=	phase change material
s	=	solid
w	=	wall

Received 29 December 2009; revision received 1 March 2010; accepted for publication 1 March 2010.

*Laboratoire de Thermique Energétique et Procédés, Avenue de l'Université, B.P. 1155; Laboratoire d'Energétique, Mécanique des Fluides et Science des Matériaux, Faculté des Sciences, B.P. 2121, 93000 Tétouan, Morocco; tarik.elrhafiki@univ-pau.fr.

†Laboratoire de Thermique Energétique et Procédés, Avenue de l'Université, B.P. 1155.

I. Introduction

IN CONVENTIONAL thermal storage systems, thermal energy is transferred by the sensible heat of a single-phase working fluid and is proportional to the source sink temperature difference. Because these systems are often operated with small temperature differences, the single-phase fluid must be pumped at a high-volume flow rate. As a result, the system consumes a large amount of pumping power. In such systems, the increase in the thermal capacity of heat transfer fluid is an important problem and is of growing concern to engineers.

Recently, researchers and engineers have investigated the effects of incorporating phase change materials (PCMs) in secondary heat transfer fluids with the objective of increasing thermal capacity in district cooling application. However, wide implementation of PCM in cooling systems has been limited by several operational factors including clogging of pipes and limited heat transfer rates in heat exchangers [1]. Recent developments have also demonstrated that encapsulation of phase change material can be applied to circumvent the problem associated with PCMs.

Encapsulations are usually classified by their size into macro- and microencapsulation. Macroencapsulation comprises the inclusion of PCM in some form of package such as tubes, pouches, spheres, panels, or other receptacles [2,3]. These containers can serve directly as heat exchangers or they can be incorporated in building products. Previous experiments with macroencapsulation failed due to the poor heat transfer rate. The PCM freezes on the heat exchanger surface, resulting in a poor heat transfer rate due to the low thermal conductivity of PCMs. To overcome this drawback, researchers have proposed various heat transfer enhancement techniques, e.g., use of partitions/fins, graphite/metal matrices, dispersed high-conductivity particles in the PCM, and microencapsulation of PCM [4].

In recent years, a new approach was proposed [5,6], in which the PCM was microencapsulated and suspended in a single-phase heat transfer fluid to form microencapsulated phase-change-material (MEPCM) slurry. MEPCM offers an opportunity to reduce weight

and volume in thermal management systems by using the high latent heat of the PCM [7–13]. Microencapsulated PCMs can also used to regulate temperature in a variety of applications. A potential drawback of microencapsulation is, however, that the chance of supercooling increases.

In previous studies, the flow and heat transfer characteristics of MEPCM slurry at laminar flow condition have been investigated by a number of researchers. Sohn and Chen [14] showed that in the case of using MEPCM with water slurries, microconvection increases with increasing Peclet number. Peclet number can be increased by increasing shear rate, particle size, and decreasing fluid thermal diffusivity. Charunyakorn et al. [15,16] conducted a numerical simulation of microencapsulated phase change suspension flow in a circular tubes and parallel plates for different boundary conditions for low temperature application. Their results showed that the heat transfer in suspension flow is dependent on the bulk Stefan number and volumetric concentration. Their model also predicts an augmentation of heat transfer coefficient by 1.5–3 times combined with 40–60% reduction in temperature rise. In Charunyakorn et al.'s model the thickness of the microcapsule's crust was ignored. To investigate the effect of microcapsule crust on the heat transfer in suspension flow, Zang and Faghri [17] proposed a numerical solution for laminar forced-convection heat transfer of a MEPCM suspension in a circular tube with constant heat flux. They solved the melting in the microcapsule using a temperature-transforming model instead of a quasi-steady model. Goel et al. [18], Choi et al. [19], Wang et al. [20], and Rao [21] conducted experimental studies to investigate the flow and the heat transfer characteristics of MEPCM flowing in metal circular tubes or in rectangular channels. The results showed that the use of MEPCM can reduce the rise in wall temperature of the tube by up to 50% as compared with a single-phase fluid with the same nondimensional parameters. Compared with single-phase fluid, using MEPCM could significantly enhance the heat transfer in suspension flow.

Several numerical and experimental studies [22,23] were conducted in order to investigate the effect of PCM on the hydraulic and thermal performance of the microchannel heat sink using PCM-water slurries as a working fluid. Xing et al. [9] used a two-phase flow, 2-D, axisymmetric model to study the performance of the liquid flow with MEPCM particles in microchannel tubes. They showed an optimal wall heat flux at specified Reynolds number where the effectiveness factor "the ratio of the total heat transfer rate of the PCM suspension flow to the total heat transfer rate of water only with the same inlet outlet temperature difference," is at a maximum due to the full melting of the PCM right at the channel outlet. The heat transfer of MEPCM in three kinds of tubes with coaxially inserted cylindrical bars was numerically investigated using equivalent specific heat model [7]. It is found that in the tubes with coaxially inserted cylindrical bars, the heat transfer effects of MEPCM become more and more pronounced with the Stefan number decreasing.

Several past studies also attempted to deal with flow and melting behaviours of MEPCM in turbulent conditions. Choi et al. [19] measured the local pressure drop and heat transfer coefficient of turbulent phase change emulsion flow (mixture of water and PCM with additive of emulsion) in horizontal tube with constant heat rates. They observed a significant enhancement in heat transfer performance due to the latent heat effect when PCM melting. Yamagichi et al. [1] measured the pressure drop and local convective heat transfer coefficients of turbulent microencapsulated octadecane slurry flow along the horizontal circular pipe with constant heating rate, and they reported that heat transfer performance of the slurry was greatly influenced by the effects of latent heat, as were those in the case reported by Choi et al. [19]. They also reported that such effect also depends upon the particle fractions, degree of turbulence, and heating rate on the tube wall.

A significant number of authors have based their work on paraffins [24]. Choi [25] has used paraffins because their melting points are at least a ew degrees greater than the carrier fluid (water). Alvarado [26] conducted a series of experiments and evaluated the thermal properties of tetradecane microcapsules with an average size of 4.4 μm. Goel et al. [18] describe experiments of MCPCMs filled with n-eicosane in which the experimental conditions were limited to laminar flow and constant heat flux.

By far the best-known PCM is water. It has been used for cold storage for more than 2000 years. Today, cold storage with ice is state of the art and even cooling with natural ice and snow is used again. For temperatures below 0°C, usually water–salt solutions with an eutectic composition are used. Water–salt solutions consist of two components, water and salt, which means phase separation could be a problem. To prevent phase separation, and to achieve a good cycling stability, eutectic compositions are used. Eutectic compositions are mixtures of two or more constituents, which solidify simultaneously out of the liquid at a minimum freezing point. Therefore, none of the phases can sink down due to a different density. Further on, eutectic compositions show a melting temperature and good storage density. The thermal conductivity of eutectic water–salt solutions is similar to that of water. Water–salt solutions are chemically very stable, but can cause corrosion to other materials like metals. Most of the salt solutions are rather safe, but should not leak in larger amounts.

A limited number of journal papers present and discuss heat transfer for microencapsulated water or aqueous solution [27,28]. The use of the aqueous solution as PCM makes the problem of the heat transfer in the suspension more complicated. The aim of this paper is to analyze the forced convective heat transfer enhancement with microencapsulated phase change slurries for laminar flow in a circular tube with constant heat flux. Two kinds of PCM are tested: water and aqueous solution. The physical model gives the opportunity to access the temperature of the suspended liquid for different positions along the axial direction of the horizontal circular duct. Several simulations were conducted to investigate the effects of different parameters such as the heat flux, the particle radius, the volume fraction of particles and the initial concentration of the aqueous solution.

II. Physical Model

We analyze the heat transfer of a MEPCM suspension flowing in a tube subjected to constant parietal heat flux. Figure 1 shows a schematic diagram describing the problem. The carrier fluid with microencapsulated PCM particles enters the test section at a temperature T_i equal to or below the phase change temperature of the PCM to ensure that all phase changes will take place in the test section. The following assumptions are made for the formulation of the governing equations:

1) The maximum fraction volume fraction of microcapsules is limited to 0.20 in order that the fluid can be considered as Newtonian.

2) The flow is assumed to be incompressible and laminar. It is also hydrodynamically fully developed.

3) The suspension is assumed to be homogeneous.

4) The microencapsulated particles are considered to be rigid inert spheres with density approximately equal to that of the suspending fluid.

5) The viscous dissipation is neglected.

6) The particle free layer next to the tube wall is assumed to be negligible.

7) The surface heat flux on the side wall is constant.

The governing equation for the energy balance of the suspension inside the duct is written in the cylindrical coordinate system and given as follows:

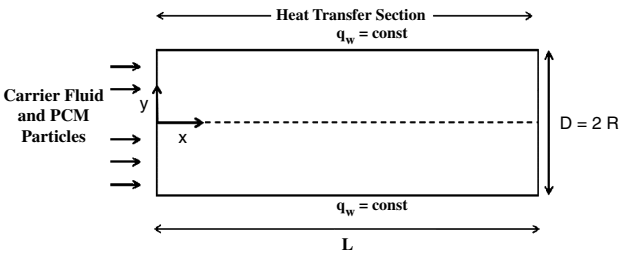

Fig. 1 Schematic diagram of fluid and MEPCM particle suspensions flowing through a circular tube under constant wall heat flux at the wall.

$$\rho c\frac{\partial T}{\partial t}+\rho cu\frac{\partial T}{\partial x}=\frac{\partial}{\partial x}\left(k_e\frac{\partial T}{\partial x}\right)+\frac{1}{y}\frac{\partial}{\partial y}\left(k_e\frac{\partial T}{\partial y}\right)+S \quad (1)$$

Since the flow is fully developed, the following laminar velocity profile is obtained from the momentum equation:

$$u=2u_m\left[1-\left(\frac{y}{R}\right)^2\right] \quad (2)$$

with the following boundary conditions:

$$T=T_i, \qquad x=0, \qquad y<R \quad (3)$$

$$\frac{\partial T}{\partial y}=0, \qquad y=0, \qquad x>0 \quad (4)$$

$$\frac{\partial T}{\partial y}=-\frac{q''_w}{k_e}, \qquad y=R, \qquad x>0 \quad (5)$$

The density and specific heat in Eq. (1) are those of the suspension and are evaluated by the weighted mean method [18]:

$$\rho=\frac{1}{\frac{\varepsilon}{\rho_{\text{pcm}}}+\frac{(1-\varepsilon)}{\rho_f}} \quad (6)$$

$$c=\varepsilon c_{\text{pcm}}+(1-\varepsilon)c_f \quad (7)$$

where ε is the volumetric concentration of suspended particles, ρ_f is the mass density of the working fluid, ρ_{pcm} is the mass density of the PCM, c_f is the specific heat of the working fluid, and c_{pcm} is the specific heat of the PCM.

The thermal conductivity k_e is an effective value that includes microconvection due to the eddy motion of fluid around the particles. Because of the enhancement created by the particle–fluid interactions, the effective conductivity of flow slurries is higher than the thermal conductivity of static dilute suspension. In our study k_e is calculated from the following formula [15]:

$$\begin{cases}\frac{k_e}{k_b}=1+B\varepsilon Pe_p^m\\ B=3, m=1.5, Pe_p<0.67\\ B=1.8, m=0.18, 0.67\le Pe_p\le 250\\ B=3, m=\frac{1}{11}, Pe_p>250\end{cases} \quad (8)$$

where k_b is the bulk thermal conductivity of the suspension. It can be evaluated from Maxwell's relation [29]:

$$\frac{k_b}{k_f}=\frac{2+\frac{k_b}{k_f}+2\varepsilon(\frac{k_b}{k_f}-1)}{2+\frac{k_b}{k_f}-\varepsilon(\frac{k_b}{k_f}-1)} \quad (9)$$

The Peclet number of the particle Pe_P found in Eq. (8) is [15]

$$Pe_p=8Pe_f\left(\frac{r_p}{R}\right)^2\left(\frac{y}{R}\right) \quad (10)$$

where $Pe_f=2Ru_m/\alpha_f$ and α_f is the thermal diffusivity of the working fluid.

The heat source function S in the energy equation (1) is the result of the phase change in the suspended microparticles. This phenomenon will be discussed in greater detail in the next sections.

III. Melting Modeling for the PCM Inside a Microparticle

The source term S represents the heat released or absorbed by the phase change process in the microparticles. It can be obtained from the sum of the heat absorbed per each particle in the unit volume of the suspension:

$$S=3h_p\varepsilon\frac{(T_{\text{pcm}}|_{r=r_P}-T)}{r_p} \quad (11)$$

where T_P is the particle temperature, T is the suspension temperature, and r_p is the particle radius. The convection heat transfer coefficient h_p between the particle and the working fluid can be further deduced from [15]

$$h_p=A_P(1+B.\varepsilon.\beta_p^m R^m) \quad (12)$$

where

$$A_p=\frac{2(1-\varepsilon)}{2-3\varepsilon^{1/3}+\varepsilon}\cdot\frac{2+\frac{k_p}{k_f}+2\varepsilon(\frac{k_p}{k_f}-1)}{2+\frac{k_p}{k_f}-\varepsilon(\frac{k_p}{k_f}-1)}\cdot\frac{k_f}{r_p}$$

The values of constants B and m depend on the particle Peclet number [see Eq. (8)].

In this investigation, local heat transfer coefficients h between the tube wall surface and suspension flow was defined as

$$h=\frac{q''_w}{(T_w-T_{\text{mean}})} \quad (13)$$

where q''_w is the local heat flux at the tube wall, which is defined as the heat rate per square meter on the internal tube pipe surface, T_w is the local inner wall surface temperature, and T_{mean} is the local bulk mean temperature of the fluid over a circular test section A_c.

The mean flow temperature is mass-weighted averaged in the test section and represented as a function of the flow direction using the following expression:

$$T_{\text{mean}}=\frac{\int_{A_c}\rho_b uc_b T\,\mathrm{d}A_c}{\int_{A_c}\rho_b uc_b\,\mathrm{d}A_c} \quad (14)$$

where $c_b=c_{\text{pcm}}.\varepsilon+c_f(1-\varepsilon)$

A. Kinetics of the Isothermal Melting Inside the Microcapsule

Figure 2 details the regions of a melting process inside the particle. The radius of the particle and the PCM core are r_p and r_i, respectively. The particle absorbs heat by convection at its outer surface. To follow the evolution of the interface liquid–solid r_s within the microcapsule, the enthalpic approach is adopted [30].

The enthalpic formulation that has been described in detail by Voller [31] rests on the partition of the volume occupied by the PCM into a finite number of control volumes and writing the energy conservation in spherical coordinated terms:

$$(\rho c)_{\text{pcm}}\frac{\partial T_{\text{pcm}}}{\partial t}=\frac{1}{r^2}\frac{\partial}{\partial r}\left(r^2k_{\text{pcm}}\frac{\partial T_{\text{pcm}}}{\partial r}\right)-\rho_{\text{pcm}}L_F\frac{\partial f}{\partial t} \quad (15)$$

where f is the liquid fraction in the particle and L_F is the latent heat of fusion.

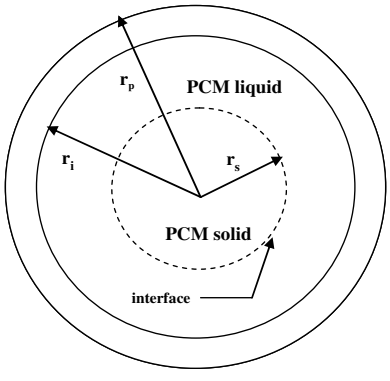

Fig. 2 Melting process in a particle.

The initial and the boundary conditions are specified by

$$T_{\text{pcm}}(r,0) = T_i \quad \text{and} \quad f(r,0) = 0 \tag{16}$$

$$\left(\frac{\partial T_{\text{pcm}}}{\partial r}\right)_{r=0} = 0 \tag{17}$$

$$-k_{\text{pcm}}\left(\frac{\partial T_{\text{pcm}}}{\partial r}\right)_{r=r_i} = \frac{T_{\text{pcm}}|_{r=r_i} - T_{\text{pcm}}|_{r=r_p}}{R_{\text{env}}} = \frac{T_{\text{pcm}}|_{r=r_p} - T}{R_f} \tag{18}$$

where R_{env} is the thermal resistance of the microcapsule's crust, R_f is the thermal resistance for convective exchange between the microcapsule's crust and the working fluid:

$$R_f = \frac{1}{4\pi r_p^2 h_p}, \qquad R_{\text{env}} = \frac{1}{4\pi k_p}\left(\frac{1}{r_i} - \frac{1}{r_p}\right) \tag{19}$$

where k_P is the thermal conductivity of the microcapsule's crust.

B. Kinetics of the Nonisothermal Melting Inside the Microcapsule

Figure 3 shows the equilibrium phase diagram for water–salt solution ($NH_4Cl - HO_2$) system. The symbols L, S, and $L + S$ denote the liquid phase, the solid phase, and the solid–liquid two-phase, respectively. The lowest temperature possible for liquid salt solution is $-15.7°C$. At that temperature, the salt begins to crystallize out of solution, along with the ice, until the solution completely freezes. The frozen solution is a mixture of separate solute crystals and ice crystals. This mixture is called eutectic mixture. If the ice, salt, and salt–water are present in the binary mixture, and their amounts are not changing over time we must be at the eutectic point ($T_E = -15.7°C$ and $X_E = 0.195$). If the solute mass fraction X_a is lower than X_E the ice mass fraction X_{ic} can be calculated from the liquidus temperature of the binary mixture solution, which is a function ofX_a:

$$T_{\text{pcm}} = T_{\text{pcm}}(X_a) \tag{20}$$

Once the initial mass fraction of solute in the binary mixture solution before freezing x_0 and temperature are known, the equilibrium ice mass fraction is calculated with the following relation:

$$X_{\text{ic}}(T_{\text{pcm}}) = 1 - \frac{x_0}{X_a(T_{\text{pcm}})} \tag{21}$$

where $X_a(T_{\text{pcm}})$ is calculated from the liquidus curve, the inverse of Eq. (20).

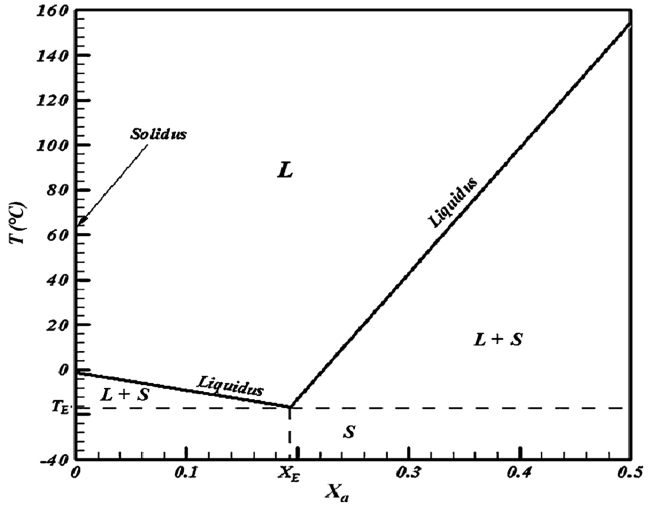

Fig. 3 Binary phase diagram NH4Cl-H2O.

To obtain the governing equations of the isothermal and nonisothermal melting of the binary mixture (i.e., the ice–water–salt solution), the following assumptions are made in formulating the governing equations:

1) The PCM temperature is assumed to be homogeneous inside the microcapsule.

2) The microcapsule's crust is negligible.

During the isothermal melting (i.e., eutectic melting $T_{\text{pcm}} = T_E$), the exchanged heat proceeds from the fraction of crystal that is melting:

$$\rho_{\text{pcm}} L_F \frac{\partial X_{\text{ic}}}{\partial t} = -\frac{3}{r_i} h_p (T - T_E) \tag{22}$$

During the nonisothermal melting (i.e., progressive melting), the appropriate energy equation for the binary mixture is

$$(\rho c)_{\text{pcm}} \frac{\partial T_{\text{pcm}}}{\partial t} = \rho_{\text{ic}} L_F \frac{\partial X_{\text{ic}}}{\partial t} + \frac{3}{r_i} h_p (T - T_{\text{pcm}}) \tag{23}$$

In the above equation, the unknowns are only the temperatures T_{pcm} because the ice mass fractions are themselves function of the temperatures according the Eq. (21).

C. Heat Exchange Before and After the Melting Process

To describe the heat exchange between the microcapsules and the working fluid before and after the melting process we assume that the PCM temperature is homogeneous in the particle. So the energy equation of the PCM inside the particle is given by

$$(\rho c)_{\text{pcm}} V_{\text{pcm}} \frac{\partial T_{\text{pcm}}}{\partial t} = \frac{T - T_{\text{pcm}}|_{r=r_i}}{R_f + R_{\text{env}}} = \frac{T - T_{\text{pcm}}|_{r=r_p}}{R_f} \tag{24}$$

where V_{pcm} is the volume of PCM inside the microcapsule.

D. Numerical Methodology

Using the control volume approach, the coupled energy equations (1) and (15) are integrated over the control volumes in the (x, y) plane and in the r direction, respectively. The time integration has been performed fully implicitly and control volumes of a uniform size and constant time steps were used. The basic principal in a numerical scheme based on a volume discretization of a grid of nodes is to arrive at a set of algebraic equations that relate the value of a dependent variable at a given node P to values at the neighboring nodes, nb, via the specification of appropriate coefficients a_P. The resulting finite difference equations are given by the following forms (where superscript o refers to the previous time-step values):

Suspension:

$$a_P T_P = a_P^o T_P^o + \sum_{nb} a_{nb} T_{nb} + b \tag{25}$$

where

$$b = 3h_p \frac{\varepsilon}{r_p} T_{\text{pcm}}(r_p, t) \tag{26}$$

PCM:

$$a_{\text{pcm},P} T_{\text{pcm},P} = a^o_{\text{pcm},P} T^o_{\text{pcm},P} + \sum_{nb} a_{\text{pcm},nb} T_{\text{pcm},nb} + b_{\text{pcm}} \tag{27}$$

where

$$b_{\text{pcm}} = \rho_{\text{pcm}} L_F (f_P(t) - f_P(t + \Delta t)) \tag{28}$$

Since the coefficients of the system to be solved are evaluated implicitly, an iterative method of resolution based on a standard Thomas algorithm was used to obtain the time varying solution to the system. During this iterative process, the liquid mass fraction f was updated at each iteration using the method described by Voller [31]: namely, for

$$T_m - \Delta T_p \prec T_{\text{pcm}} \prec T_m : \; f_P^{n+1} = f_p^n + \frac{a^n_{\text{pcm},P}}{\rho^n_{\text{pcm}} L_F}(T^n_{\text{pcm},P} - T_m) \tag{29}$$

where T_m is the melting temperature and ΔT_p is the phase change temperature range. The index n corresponds to the current iteration loop. It is interesting to note that the parameter ΔT_p is used only when the melting process will not occur exactly at the melting point, but instead will take place over a temperature range below the melting point of the PCM.

At each node the liquid fraction will be corrected using the following expressions:

$$f_P^{n+1} = \begin{pmatrix} 0 \text{ if } f_P^{n+1} < 0 \\ 1 \text{ if } f_P^{n+1} > 0 \end{pmatrix} \tag{30}$$

Further details concerning the numerical implementation of the present enthalpic phase change method may be found in the work of Voller [31]. At each time step, convergence was assumed to be reached as soon as the temperature residuals fell below some predefined values tol and tol_{pcm}:, i.e.,

$$\left|\frac{T_P^{n+1} - T_P^n}{T_P^n}\right| < \text{tol}$$

and

$$\left|\frac{T^{n+1}_{\text{pcm},P} - T^n_{\text{pcm},P}}{T^n_{\text{pcm},P}}\right| < \text{tol}_{\text{pcm}}$$

After performing preliminary tests aimed at determining the sensitivity of the results to the value of tol and tol_{pcm}, all simulations were conducted with $\text{tol} = \text{tol}_{\text{pcm}} = 10^{-5}$.

The finite volume discretization of the energy equation (23) cannot be directly accomplished, because it contains as unknowns both the temperature and the ice mass fraction. A fully time implicit integration of Eq. (23) with mass lumping of the source term and transient terms gives

$$a_{\text{pcm},P} T^{n+1}_{\text{pcm},P} = a^o_{\text{pcm},P} T^o_{\text{pcm},P} + (X^o_{\text{ic}} - X^{n+1}_{\text{ic}}) \tag{31}$$

Following Swaminathan and Voller [32] the current iterate of the ice mass fraction can be approximated as

$$X^{n+1}_{\text{ic}} = X^n_{\text{ic}} + \frac{\mathrm{d}X_{\text{ic}}}{\mathrm{d}T}(T^{n+1}_{\text{pcm}} - T^n_{\text{pcm}}) \tag{32}$$

where the term $\mathrm{d}X_{\text{ic}}/\mathrm{d}T$ can be evaluated by deriving Eq. (21) at T^n_{pcm}

$$\frac{\mathrm{d}X_{\text{ic}}}{\mathrm{d}T} = \frac{x_0}{X_a^2}\frac{\mathrm{d}X_a}{\mathrm{d}T} \tag{33}$$

and $\mathrm{d}X_a/\mathrm{d}T$ is the derivation of the liquidus.

IV. Results and Discussion

Results from three kinds of microencapsulated PCM dispersed in propylene–glycol–water mixture 40% are tested in this paper. The first case deals with the melting of the phase change suspension with n-eicosane particles, for which experimental results exist, to demonstrate the reliability of the physical model. In the second case we present the results for water as microencapsulated PCM. The third case investigates the convective heat transfer enhancement with microencapsulated binary mixture (ice–water–NH_4Cl).

A. Validation of the Numerical Model for the Melting Process

To validate the reliability of the physical model the melting of the MEPCM suspension flowing in a horizontal tube is investigated. The results are compared with the experimental data of Goel et al. [18]. The same parameters as those given in [18] are chosen in the following computation: wall heat flux $q_w = 3$ kW, radius and length of the tube $R = 1.57$ mm and $L = 314$ mm (Fig. 1), microencapsulation radius of n-eicosane $r_p = 50$ μm, volume fraction of microparticles $\varepsilon = 10\%$, bulk Stefan number $Ste = 1$, and Reynolds number $Re = (2u_m R\rho/\mu) = 200$, where μ is the viscosity of a Newtonian suspension given by the following expression [33]:

$$\mu = \mu_f(1 - \varepsilon - 1.16\varepsilon^2)^{-2.5} \tag{34}$$

For comparison with the experimental results of Goel et al. [18], our results are presented with the same dimensionless wall temperature

$$T_{wx} = \frac{T_w - T_i}{q''_w R/k_b}$$

and dimensionless axial distance along the tube $x^* = x/RePrR$, as in [18].

Because of the existence of the supercooling phenomena in the freezing process, the PCM in the microcapsules may not be in a completely solid state when the suspension enters the test section [18]. Therefore, the amount of heat absorbed by the microcapsules would be decreased. To simulate this phenomenon, the melting process can be assumed to take place over a range of temperatures below the melting point of the PCM. Several phase change temperature ranges ΔT_P are used to calculate the heat transfer in the microencapsulated PCM suspensions. The effects of a varying range of the phase change temperature difference ΔT_P on the tube wall temperature is investigated and illustrated in Fig. 4a. Three values of ΔT_P were studied: 0.6, 1.6 and 2.1°C. As shown in Fig. 4a, the small difference between numerical prediction and experimental data is obtained for $\Delta T_P = 2.1$°C, which means that the melting takes place over a range of temperatures from 34.1°C to 36.5°C. However, this range of phase change temperatures should be examined and established by further experimental work, in order to find an accordingly appropriate value of ΔT_P that can be used in the mathematical model. The differences between the present prediction and the experimental data near the inlet and the exit of the tube can be attributed to the effect of pipe wall conduction associated with the relatively thick copper pipe used in the experiment [18]. Another possible reason for the discrepancy lies in the assumptions used in the proposed model. In fact, the PCM in Goel et al.'s [18] experiments was encapsulated in a crust that made up 30% of the total volume of the microcapsule (the PCM volume was reduced to 70%), but in our model the PCM was supposed to be encapsulated in a crust that made up 5% of the total volume of the microparticle. Figure 4b presents the effect of the microcapsule crust on dimensionless wall temperature. As can be seen, the tube wall temperature was significantly increased when the microcapsule had a crust. In other words the effect of microcapsules is reduced by the thermal resistance of the crust. We can note that the difference between the numerical result and the experimental data can be significantly decreased by varying the thermal resistance of the crust.

B. Isothermal Melting

In this part, the numerical investigation was focused on the thermal fully developed region. The microencapsulated phase-change-material slurry was made of pure ice. Propylene–glycol–water mixture 40% was chosen as a carrier fluid. The tube length of $L = 0.45$ m $(L/D = 100)$ is used in the computation. The parameters for the present problem are the wall heat flux, the bulk Stefan number, the volumetric particle concentration, the Reynolds number, and the particle diameter.

1. *Effect of Wall Heat Flux*

Figure 5 shows the variation of the wall temperature of the cylindrical tube as a function of the distance from the inlet tube for different wall heat fluxes: $q_w = 200$, 400, and 800 W. We note that the wall temperature of the duct increases by increasing the heat flux. The evolutions of T_w are not linear due to the variable specific heat of the suspension caused by the absorption of energy associated with PCM melting. The rupture of the monotonic decrease in the wall temperature evolution is related to the phase change process. We can also note that the duration of the phase change process decreases by

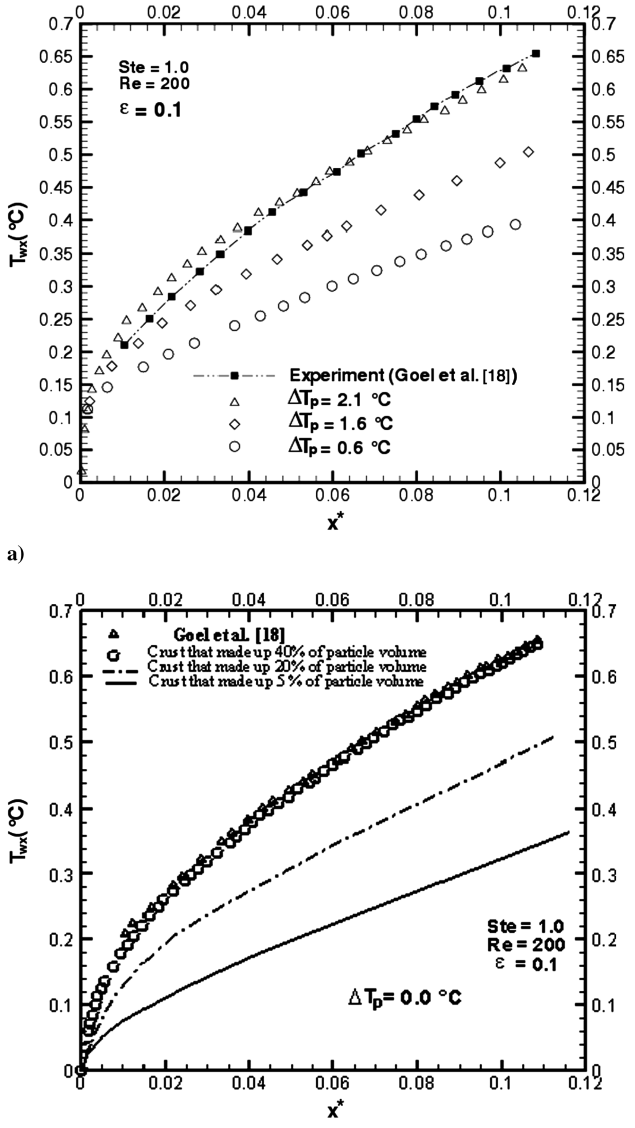

Fig. 4 Plots of a) tube wall temperature for different phase change temperature ranges ΔT_P and comparison with the experimental results of Goel et al. [18] and b) effect of the microcapsule crust on dimensionless wall temperature and comparison with the experimental results of Goel et al. [18].

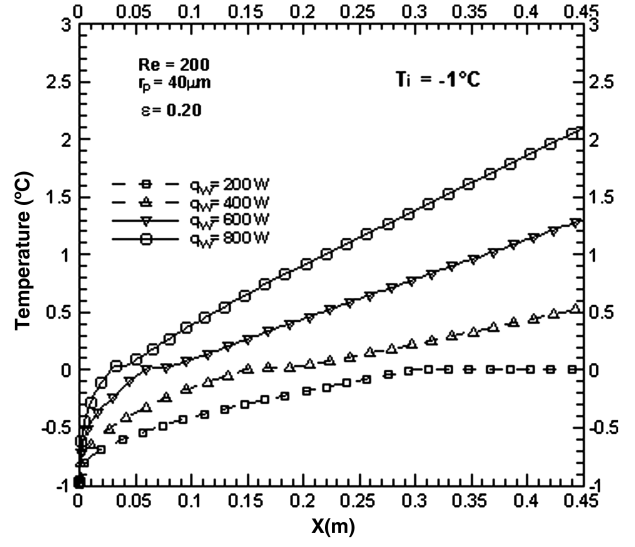

Fig. 5 Effect of heat flux on wall temperature ($Ste = 0.1$).

increasing the heat flux. From a practical point of view, this observation indicates the existence of an optimal relation among the heat flux, PCM volume fraction, tube geometric parameters, and Reynolds number, such that a significant increase in heat transfer between the suspension and the wall tube occurs while maintaining a melting region throughout the horizontal tube.

Figure 6 shows the local heat transfer coefficient of the suspension as a function of the distance from the inlet tube for various heat fluxes. In the melting region, the suspension temperature remains at the phase change temperature, preventing both fluid and PCM temperature from increasing. It is also causes the local heat transfer coefficient to increase in the melting region and to reach the peak value at the location where the mean temperature of the particle phase reaches the melting temperature. Such characteristics can be explained clearly from examination of the wall temperature profile development. During the phase change process, $T_w - T_{\text{mean}}$ decreases and the local heat transfer coefficient increases until it reaches a maximum.

2. *Effect of the Stefan Number*

The most pertinent nondimensional group of parameters for the description of the phase change process is the bulk Stefan number, defined here by the following expression:

$$Ste = \frac{\rho_b c q''_w R}{\rho_{\text{pcm}} k_b \varepsilon L_F} \tag{35}$$

The Stefan number, which is used to characterize phase change problems, represents the ratio of the sensible heat capacity of the suspension to its latent heat capacity. For constant wall heat flux, the sensible heat capacity of the suspension is defined in terms of the absolute value of the characteristic temperature. Bulk Stefan numbers of 0.1, 0.5 and 1.0 were considered in this study.

As shown in Fig. 7, the bulk Stefan number Ste is an important parameter that strongly affects the local wall temperature in the MEPCM suspension, because a lower Stefan number indicates a higher latent heat of fusion L_f by comparison to the specific heat capacity c of the suspension for the same phase change temperature range.

3. *Effect of the Volume Fraction of the Microparticles*

The volumetric concentration of the microparticles is another parameter that influences the heat transfer enhancement in phase change slurries because ε affects not only the value of specific heat capacity of the suspension, but also the value of the effective thermal conductivity. A higher concentration of microparticles implies a

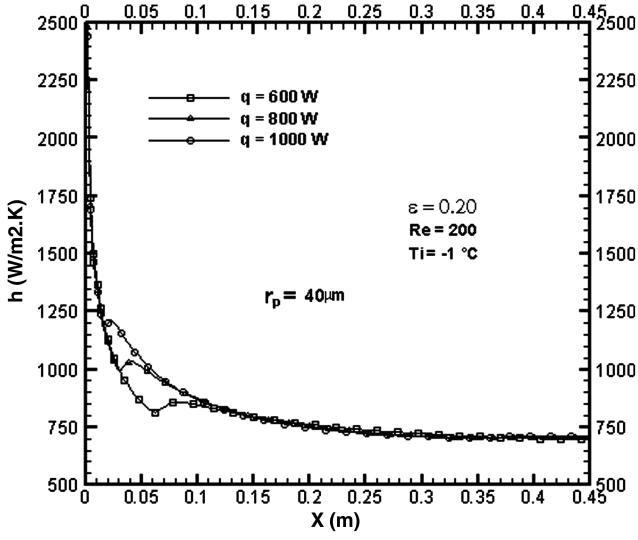

Fig. 6 Effect of heat flux on the local heat transfer coefficient ($Ste = 0.1$).

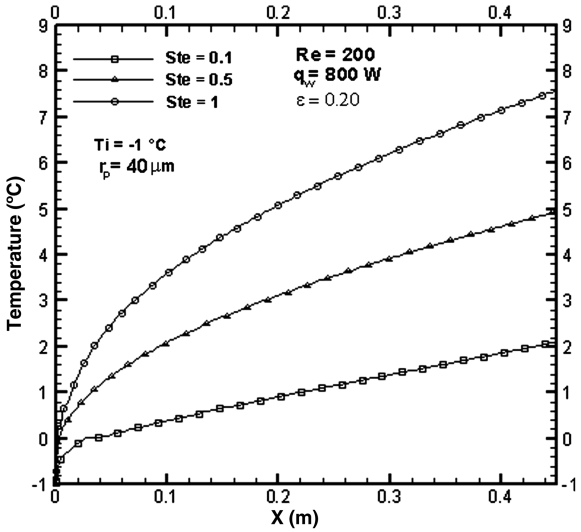

Fig. 7 Effect of Stefan number on wall temperature.

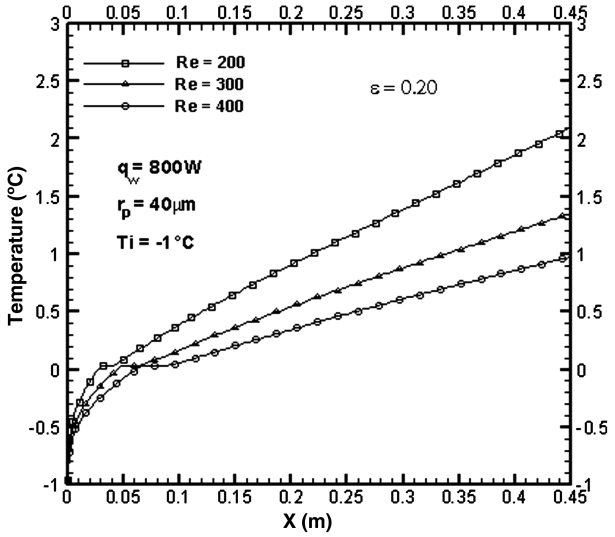

Fig. 9 Effect of Reynolds number on wall temperature (*Ste* = 0.1).

higher energy-storage capability. We can notice in Fig. 8 that the wall temperature increases when the volumetric concentration is lower. We can also notice that the degree of heat transfer enhancement in the thermally fully developed region is much larger than that in the thermal entry region, because for a single-phase fluid the heat transfer is stronger in the entry region than in the thermally developed region.

However, it is important to note that the volume fraction of microparticles plays an indirect role on heat transfer through the bulk Stefan number. From the definition of the Stefan number it is clear that for a given duct geometry, fluid and phase change material, its value depends only on the ratio of the wall heat flux to the volumetric concentration. Thus, for best cooling results a low Stefan number should be maintained as far as possible and concentration should be increased only if the heat flux increases.

4. Effect of the Reynolds Number on Heat Transfer

It is obvious that the fluid flow rate has an important impact on the residence time of the particles inside the tube and their rate of melting at the tube outlet. The flow rate is also involved in the calculation of the effective thermal conductivity through the Peclet number.

We show in Fig. 9 the impact of the Reynolds number on the temperature of the tube wall. Higher temperatures are obtained for lower Reynolds number. The inflection points in the curves correspond roughly to the positions of the start of melting on the tube wall. From this point, the wall temperature increases with a steeper slope following the x position; this effect is due to the change in the value of the specific heat of the PCM.

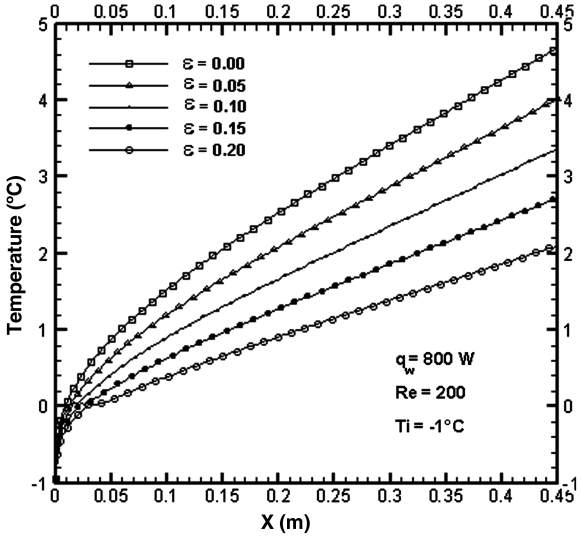

Fig. 8 Effect of ε on wall temperature (*Ste* = 0.1).

5. Effect of Particle Diameter on Heat Transfer

For cylindrical ducts filled with microparticles, the heat transfer between the suspension and the wall duct increased with decreasing particle diameter. The opposite trends result from the competing factors of the mixing effect (thermal dispersion) and the decreased contact surface area between particles as the particle diameter increases.

The effect of particle diameter on the convective heat transfer is much more complicated. Jiang et al. [34] theoretically and numerically analyzed the effect of particle diameter on the convective heat transfer. The results showed that the convective heat transfer coefficient can decrease or increase as the particle diameter increases depending on the values of the following parameters: ε, k_{pcm}, k_f, u_m, etc. A criterion for judging the effect of the particle diameter on the convection heat transfer was presented in [35]. This criterion is based on an earlier work concerning a thermal dispersion conductivity model. Jiang et al. [35] presented a new modified dispersion conductivity model. A modified approximate criterion was then developed. When the term

$$\rho u_m d > 0.787 \frac{k_e^{0.582}}{c_f} \frac{\varepsilon}{1-\varepsilon}$$

the convection heat transfer between the suspension and the wall tube increases as the particle diameter increases. Otherwise, the heat transfer increases as d decreases. The validity of this criterion was analyzed in the present study (see Figs. 10 and 11).

We can also note that the reduction of the capsule diameter induces an increase in the number of capsules and an increase in the heat transfer area and hence the heat transfer between fluid and capsules increases. As the diameter value increases the time required for latent storage increases because the heat transfer between the PCM and the coolant fluid decreases. To control the wall temperature, it is interesting to increase the capsule diameter. In reality, in industrial applications, it is difficult to reduce the capsule diameter by keeping the volume fraction of microencapsulated particles as constant.

From the results obtained, we note that the particle diameter affects the wall temperature of the duct, but the observed effect is less pronounced than those given by the evolution of the Stefan number and those concerning the variation in the volumetric concentration of the particles.

C. Isothermal and Nonisothermal Melting (Ice–Water–Salt Solution)

In this section the numerical investigation was focused on the transient regime. The microencapsulated phase-change-material

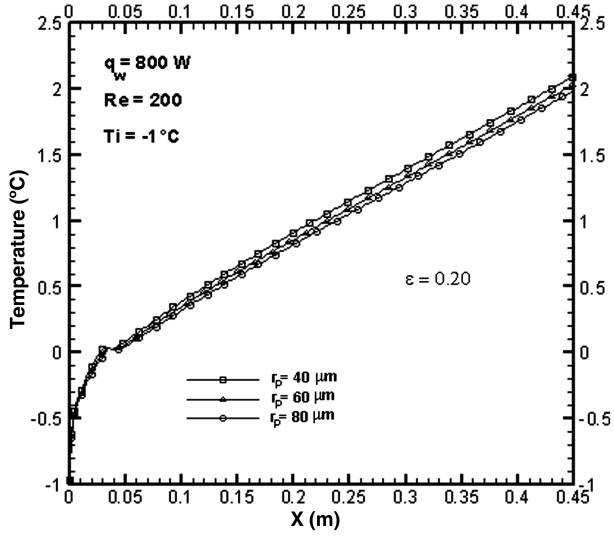

Fig. 10 Effect of r_p on the wall temperature ($Ste = 0.1$).

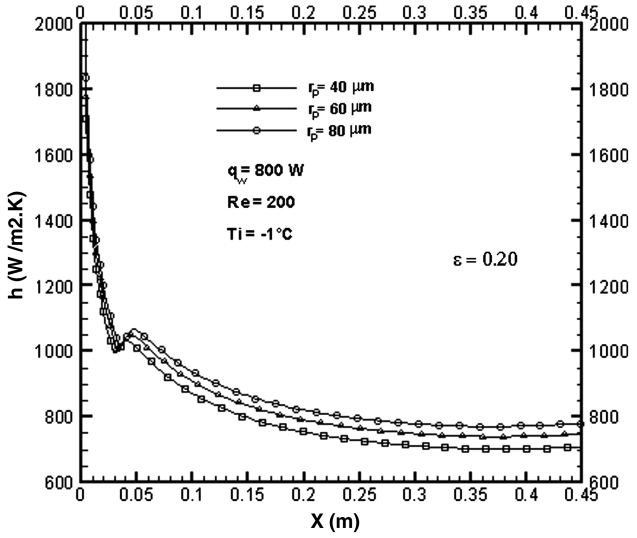

Fig. 11 Effect of r_p on the heat transfer enhancement ($Ste = 0.1$).

slurry consists of the binary mixture (ice–water–NH_4Cl). Propylene–glycol–water mixture 40% was chosen as a carrier fluid. The parameters for the present problem are the volumetric particle concentration and the initial concentration of the binary mixture. The influences of the above factors on the heat transfer inside the circular tube are clarified.

Figure 12 exhibits a temperature curve of a eutectic mixture during the melting process. This curve presents isothermal eutectic and nonisothermal solid–liquid transition. Figure 13 shows a typical plot of the fractional transformation χ curve of a simple eutectic mixture. The fractional transformation represents the reaction fraction of solid–liquid equilibrium transition.

Figure 14 shows the local wall temperature of the circular tube versus time for different volume fraction of microencapsulated particles at $x = L/2$. We note that the local wall temperature increases with decreasing volume fraction of particles. To control the wall temperature of the exchanger it is interesting to increase the volume fraction of microencapsulated in the suspension. We can also note that during the eutectic melting, heat transfer coefficient increases to reach a maximum value and thereafter decreases gradually to reach a minimum value and then increases until the maximum value is reached and thereafter remains constant during the progressive melting (see Fig. 15). Before the end of the progressive fusion the heat transfer coefficient decreases to reach a minimum

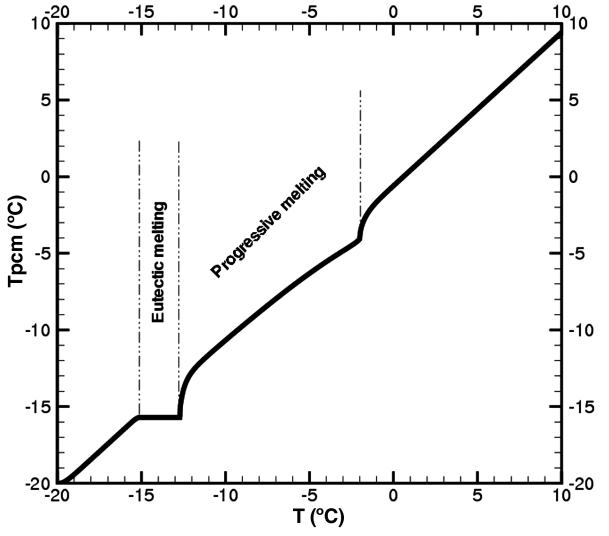

Fig. 12 Typical temperature curve of a simple eutectic mixture: eutectic and progressive melting.

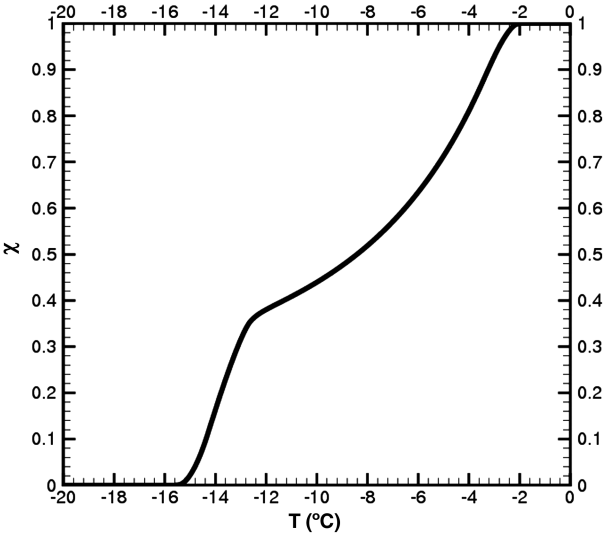

Fig. 13 Typical fraction transformation curve of a simple eutectic mixture: eutectic and progressive melting.

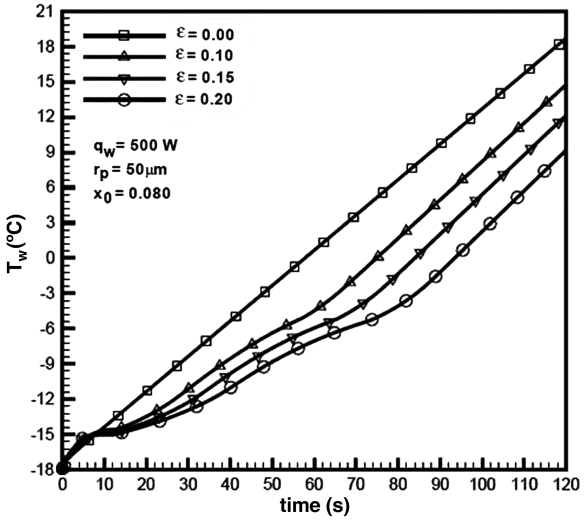

Fig. 14 Variation of local wall temperature for various volume fraction of particles ($x = L/2$,$Ti = -18°C$, and $Re = 200$).

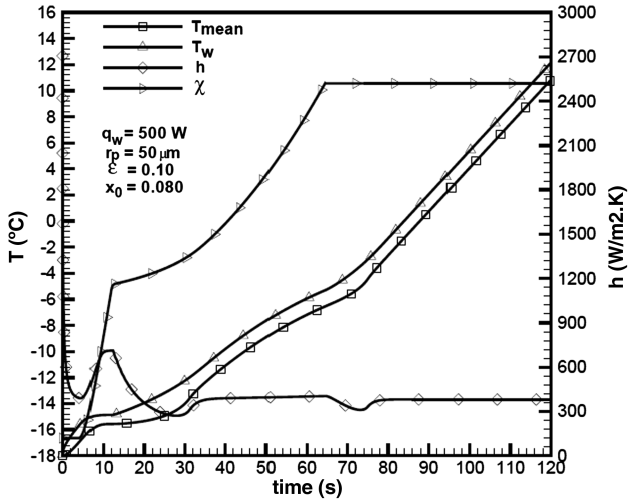

Fig. 15 Evolution of the local heat transfer coefficient, the wall temperature, the mean temperature of the suspension and the liquid fraction at $x = L/2$versus time ($Ti = -18°C$, $Ste = 0.1$, and $Re = 200$).

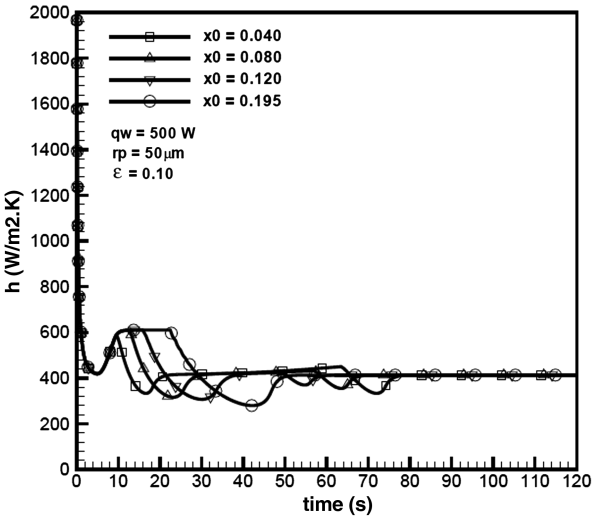

Fig. 17 Effect of the initial mass fraction of the solute on the local heat transfer coefficient ($x = L/2$, $Ste = 0.1$, and $Re = 200$).

value and thereafter increases until it reaches a maximum value and finally stabilized by indicating the end of the progressive melting. The heat transfer coefficient variation reflects the difference between the wall temperature and the suspension temperature. These temperatures are influenced by the kinetic of the phase change process during the eutectic and progressive melting inside the particles.

To study the effect of the initial concentration of the binary mixture on the local wall temperature of the circular tube, we have tested four flows with different initial concentrations at$x = L/2$ (see Figs. 16 and 17). We note that the tube wall temperature and the local heat transfer coefficient depend on the initial concentration of the solute. We observe that the eutectic melting of the binary mixture becomes faster when the initial concentration of the solution decreases. It is interesting to note that the use of the eutectic solution ($x_0 = X_E$) allows a better control of the tube wall temperature. This can be explained by the fact, that during the eutectic melting, the eutectic solution absorbs an important latent heat compared with the noneutectic solution (see Fig. 18).

V. Conclusions

A physical model is proposed for predicting the laminar hydrodynamic and heat transfer characteristics of suspension flow

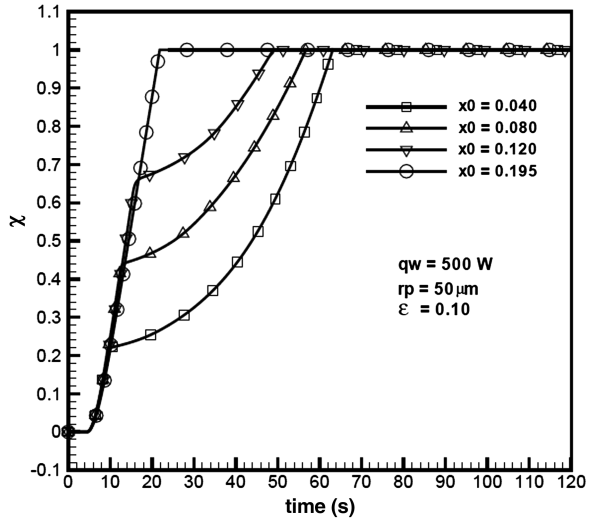

Fig. 18 Evolution of the liquid fraction at $x = L/2$versus time for various initial mass fraction of the solute ($Ti = -18°C$, $Ste = 0.1$, and $Re = 200$).

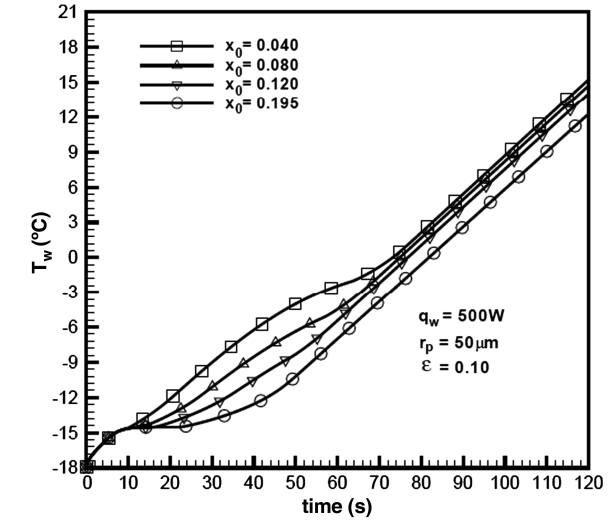

Fig. 16 Effect of the initial mass fraction of the solute on the tube wall temperature ($x = L/2$, $Ti = -18°C$, and $Re = 200$).

with microencapsulated phase change material in a circular duct under constant wall heat flow. Heat absorption due to the isothermal and nonisothermal melting in the particles was included in the energy equation as a heat source. The wall temperature of the circular tube and the local heat transfer coefficient were calculated and reported. It is found that the microencapsulated phase change material can be used to regulate the wall temperature of the exchanger. It is also found that in the case of the binary mixture solution, the heat transfer was influenced by the initial mass fraction of the solute. The use of the eutectic solution ($x_0 = X_E$) allows a better control of the wall temperature.

Acknowledgment

This work has been completed with the support of the Inter Universitaire Franco–Marocain committee in the framework of the integrated action Volubilis (no. MA/06/152).

References

[1] Yamagishi, Y., Takeuchi, H., Pyatenko, A. T., and Kayukawa, N., "Characteristics of MPCM Slurry as a Heat Transfer Fluid," *AIChE Journal*, Vol. 45, No. 4, 1999, pp. 696–707. doi:10.1002/aic.690450405

[2] Kousksou, T., Elrhafiki, T., Arid, A., Schall, E., and Zeraouli, Y., "Power, Efficiency and Irreversibility Analysis of Latent Energy System," *Journal of Thermophysics and Heat Transfer*, Vol. 22, No. 2, 2008, pp. 234–239. doi:10.2514/1.31227

[3] Kousksou, T., Bédécarrats, J. P., Dumas, J. P., and Mimet, A., "Dynamic Modelling of the Storage of an Encapsulated Ice Tank," *Applied Thermal Engineering*, Vol. 25, No. 10, 2005, pp. 1534–1548. doi:10.1016/j.applthermaleng.2004.09.010

[4] Zalba, B., Marin, J. M., Cabeza, L. F., and Mehlin, H., "Free-Cooling of Building with Phase Change Materials," *International Journal of Refrigeration*, Vol. 27, No. 8, 2004, pp. 839–849. doi:10.1016/j.ijrefrig.2004.03.015

[5] Chen, B., Wang, X., Zeng, R. Y., Zhang, X., Wang, Niu, J., Li, Y., and Di, H., "An Experimental Study of Convective Heat Transfer with Microencapsulated Phase Change Material Suspension: Laminar Flow in a Circular Tube Under Constant Flux," *Experimental Thermal and Fluid Science*, Vol. 32, No. 8, 2008, pp. 1638–1646. doi:10.1016/j.expthermflusci.2008.05.008

[6] Wang, X., Niu, J., Li, Y., Wang, X., Chen, B., Zeng, R., Song, Q., and Zhang, Y., "Flow and Heat Transfer Behaviors of Phase Change Material Slurries in a Horizontal Circular Tube," *International Journal of Heat and Mass Transfer*, Vol. 50, Nos. 13–14, 2007, pp. 2480–2491. doi:10.1016/j.ijheatmasstransfer.2006.12.024

[7] Yamagishi, Y., Takeuchi, H., and Pyatenko, A. T., "Characteristics of Microencapsulated PCM Slurry as a Heat-Transfer Fluid," *AIChE Journal*, Vol. 45, No. 4, 1999, pp. 696–707. doi:10.1002/aic.690450405

[8] Hideo, I., Myoung-Jun, K., and Akihiko, H., "Melting Heat Transfer Characteristics of Microencapsulated Phase Change Material Slurries with Plural Microcapsules Having Different Diameters," *Journal of Heat Transfer*, Vol. 126, No. 4, 2004, pp. 558–565. doi:10.1115/1.1773584

[9] Xing, K. Q., Tao, Y. X., and Hao, Y. L., "Performance Evaluation of Liquid Flow with PCM Particles in Micro-Channels," *Journal of Heat Transfer*, Vol. 127, No. 8, 2005, pp. 931–940. doi:10.1115/1.1929783

[10] Jian, J., Peiqing, L., and Guiping, L., "Numerical Simulation of Heat Transfer of Latent Functionally Thermal Fluid in Tubes with Coaxially Inserted Cylindrical Bars in Laminar," *Science in China, Series E: Technological Sciences*, Vol. 51, No. 8, 2008, pp. 1232–1241. doi:10.1007/s11431-008-0138-1

[11] Bai, F., and Lu, W. Q., "Enhanced Heat Transfer Analysis of Latent Functionally Thermal Fluid," *Heat Transfer, Asian Research*, Vol. 33, No. 6, 2004, pp. 383–392. doi:10.1002/htj.20025

[12] Hart, R., and Thornton, F., "Microencapsulation of Phase Change Materials," Ohio Dept. of Energy, Rept. 82-80, Columbus, OH, 1982.

[13] Sabbah, R., Farid, M. M., and Al-Hallaj, S., "Micro-Channel Heat Sink with Slurry of Water with Micro-Encapsulated Phase Change Material: 3D-Numerical Study," *Applied Thermal Engineering*, Vol. 29, No. 2–3, 2009, pp. 445–454. doi:10.1016/j.applthermaleng.2008.03.027

[14] Sohn, C. W., and Chen, M. M., "Micro-Convective Thermal Conductivity in Disperse Two-Phase Mixtures as Observed in a Low Velocity Coquette Flow Experiment," *Journal of Heat Transfer*, Vol. 103, No. 1, 1981, pp. 47–51. doi:10.1115/1.3244428

[15] Charunyakorn, P., Sengupta, S., and Roy, S. K., "Forced Convection Heat Transfer in Microencapsulated Phase Change Materials Slurries: Flow Between Parallel Plates," *Phase Change and Convective Heat Transfer*, Vol. 129, American Society of Mechanical Engineers, Heat Transfer Div., 1990, pp. 55–62.

[16] Charunyakorn, P., Sengupta, S., and Roy, S. K., "Forced Convection Heat Transfer in Microencapsulated Phase Change Materials Slurries: Flow in Circular Ducts," *International Journal of Heat and Mass Transfer*, Vol. 34, No. 3, 1991, pp. 819–835. doi:10.1016/0017-9310(91)90128-2

[17] Zhang, Y. W., and Faghri, A., "Analysis of Forced Convection Heat Transfer in Microcapsulated Phase Change Material Suspensions," *Journal of Thermophysics and Heat Transfer*, Vol. 9, No. 4, 1995, pp. 727–732. doi:10.2514/3.731

[18] Goel, M., Roy, S. K., and Sengupta, S., "Laminar Forced Convection Heat Transfer in Microencapsulation Phase Change Material Suspension," *International Journal of Heat and Mass Transfer*, Vol. 37, No. 4, 1994, pp. 593–604. doi:10.1016/0017-9310(94)90131-7

[19] Choi, E., Cho, Y. I., and Lorsch, H. G., "Forced Convection Heat Transfer with Phase-Change Material Slurries: Turbulent Flow in a Circular Tube," *International Journal of Heat and Mass Transfer*, Vol. 37, No. 2, 1994, pp. 207–215. doi:10.1016/0017-9310(94)90093-0

[20] Wang, X. C., Niu, J. L., and Li, Y., "Flow and Heat Transfer Behaviors Of Phase Change Material Slurries in a Horizontal Circular Tube," *International Journal of Heat and Mass Transfer*, Vol. 50, Nos. 13–14, 2007, pp. 2480–2491. doi:10.1016/j.ijheatmasstransfer.2006.12.024

[21] Rao, Y., *An Experimental Study of Microencapsulated Phase Change Material Suspension Flow and Heat Transfer in Rectangular Minichannels*, Beijing Univ. of Aeronautics & Astronautics, Beijing, PRC, 2006.

[22] Hu, X., and Zhang, Y., "Novel Insight and Numerical Analysis of Convective Heat Transfer Enhancement with Microencapsulated Phase Change Material Slurries: Laminar Flow in a Circular Tube with Constant Heat Flux," *International Journal of Heat and Mass Transfer*, Vol. 45, No. 15, 2002, pp. 3163–3172. doi:10.1016/S0017-9310(02)00034-0

[23] Choi, E., Cho, Y. I., and Lorsch, H. G., "Forced Convection Heat Transfer with Phase Change Material Slurries: Turbulent Flow in a Circular Tube," *International Journal of Heat and Mass Transfer*, Vol. 37, No. 2, 1994, pp. 207–215. doi:10.1016/0017-9310(94)90093-0

[24] Alvarado, J. C., Marsh, C., Sohn, G., and Phetteplace, T. Newell, "Thermal Performance of Microencapsulated Phase Change Material Slurry in Turbulent Flow Under Constant Heat Flux," *International Journal of Heat and Mass Transfer*, Vol. 50, Nos. 9–10, 2007, pp. 1938–1952. doi:10.1016/j.ijheatmasstransfer.2006.09.026

[25] Choi, E., "Forced Convection Heat Transfer with Water and Phase Change Materials Slurries: Turbulent Flow in Circular Tube," Ph.D. Thesis, Drexel Univ., Philadelphia, 1993.

[26] Alvarado, J. L., "Thermal Performance of Microencapsulated Phase Change Material Slurry," Ph.D. Thesis, Univ. of Illinois at Urbana–Champaign, Urbana, IL, 2004.

[27] Jamil, A., Kousksou, T., Zeraouli, Y., and Dumas, J. P., "Liquidus Temperatures Determination of the Dispersed Binary System," *Thermochimica Acta*, Vol. 471, Nos. 1–2, 2008, pp. 1–6. doi:10.1016/j.tca.2008.02.003

[28] Kousksou, T., Jamil, A., Zeraouli, Y., and Dumas, J. P., "Equilibrium Liquidus Temperatures of Binary Mixtures from Differential Scanning Calorimetry," *Chemical Engineering Science*, Vol. 62, No. 23, 2007, pp. 6516–6523. doi:10.1016/j.ces.2007.07.008

[29] Maxwell, J. C., *A Treatise on Electricity and Magnetism*, Vol. 1, Dover, New York, 1954, pp. 440–441.

[30] Alexiades, V., and Solomon, A. D., *Mathematical Modeling of Melting and Freezing Processes*, Taylor and Francis, Washington, D.C., 1993.

[31] Voller, V. R., "Fast Implicit Finite Difference Method for the Analysis of Phase Change Problems," *Numerical Heat Transfer*, Vol. 17, No. 2, 1990, pp. 155–169. doi:10.1080/10407799008961737

[32] Swaminathan, C. R., and Voller, V. R., "Towards a General Numerical Scheme for Solidification Systems," *International Journal of Heat and Mass Transfer*, Vol. 40, No. 12, 1997, pp. 2859–2868. doi:10.1016/S0017-9310(96)00329-8

[33] Vand, V., "Theory of Viscosity of Suspensions Rigid Spheres," *Nature*, Vol. 155, 1945, pp. 364–365. doi:10.1038/155364b0

[34] Jiang, P. X., Wang, Z., Ren, Z. P., and Wang, B. X., "Experimental Research of Fluid Flow and Convection Heat Transfer in Plate Channels Filled with Glass or Metallic Particles," *Experimental Thermal and Fluid Science*, Vol. 20, No. 1, 1999, pp. 45–54. doi:10.1016/S0894-1777(99)00030-8

[35] Jiang, P. X., Ren, Z. P., and Wang, B. X., "Numerical Simulation of Forced Convection Heat Transfer in Porous Plate Channels Using Thermal Equilibrium and Non-Thermal Equilibrium Models," *Numerical Heat Transfer, Part A, Applications*, Vol. 35, No. 1, 1999, pp. 99–113. doi:10.1080/104077899275399